Aerodynamic admittance functions of bridge deck sections by CWE

L. Bruno[a], F. Tubino [b], G. Solari [b]

[a] Politecnico di Torino, Dipartimento di Ingegneria Strutturale e Geotecnica, Torino
[b] Università di Genova, Dipartimento di Ingegneria Strutturale e Geotecnica, Genova

ABSTRACT

The present paper analyses the capability of the proposed modified indicial approach in determining by Computational Wind Engineering aerodynamic admittance functions of streamlined and bluff bodies characterized by finite thickness. The former is examined in order to compare the gust response of a real wing profile Naca 0012 with the one of the ideal thin airfoil described by the well known Sears function. The latter is taken into account to pursue two main objectives. Firstly, the extension to bluff bodies of the aerodynamic admittance concept is discussed. Secondly, the capability of computational tools in predicting the aerodynamic admittance function is analysed.

KEYWORDS: Aerodynamic admittance function, Bridge aerodynamics, Computational Wind Engineering, Indicial function.

1. INTRODUCTION

The aerodynamic loads on a motionless rigid body immersed in a turbulent flow are commonly expressed in the frequency domain as linear functions of the spectral content of the incoming turbulence field and the transfer function is called aerodynamic admittance. Of course, the more aerodynamic information about the body are included in the aerodynamic admittance function, the better is the prediction of the buffeting forces.

Such approach has been widely used in the aeronautical field since the works of Küssner (1931) and Sears (1938). The latter obtained the aerodynamic admittance function relating the lift force and the vertical component of velocity for an infinitely thin streamlined section in inviscid flow. In these conditions, the superposition principle of flow patterns holds and the thin airfoil theory can be applied to obtain in closed form the so-called Sears function.

The same approach has been extended to Wind Engineering by Davenport (1962), who first introduced six aerodynamic admittance functions, relating drag, lift and moment to longitudinal and vertical turbulence components. It is worth to point out that the extension of the concept of aerodynamic admittance function to bluff body aerodynamics is not immediate and its significance deeply changes with respect to the thin airfoil.

If the body is streamlined, aerodynamic admittance function takes into account the lack of correlation of the velocity fluctuations in the region of flow affecting the body. Under the above mentioned Sears' assumptions, only the lack of correlation along the longitudinal axis is to be quantified by the aerodynamic admittance function. In principle, in case of 2-dimensional streamlined bodies with finite depth/width ratio, also the lack of correlation along the transverse direction and the effects of the curvature of the wall are to be taken into account.

If the body is bluff, its aerodynamic behaviour is deeply influenced by the separation of the boundary layer generally involving vortex shedding. In case of elongated cross-sections the

boundary layer reattaches on the side surfaces and the vortices shed at the trailing edge are convected along the same surfaces. Two main aspects are worth of discussion.
First, a part of the body lies in its own wake and it is subjected to a further component of the fluctuating force due to what is commonly called signature turbulence, in addition to the one induced by the incoming turbulence. This phenomenon can be called self-buffeting, in analogy with both the wake buffeting and the buffeting involved by the incoming eddies. It follows that aerodynamic admittance functions for bluff bodies take into account not only the lack of correlation of the incoming turbulence fluctuations, but also the effects of the signature turbulence. Hence aerodynamic admittance functions deeply depend also on the shedding process, i.e. on the incoming flow conditions and on the section geometry.
Secondly, the rate of change of the aerodynamic properties of streamlined bodies and thus their aerodynamic admittance functions do not depend on the incoming flow characteristics and the hypothesis of linearity of the aerodynamic operator holds. On the contrary, the pattern of separated flow around bluff bodies can be very sensitive to the characteristics of the incoming flow. In particular, the frequency content of the self-buffeting forces can be strongly redistributed so that the spectrum of the conventional signature turbulence varies. Hence, the linear dependence of the buffeting forces on the incoming flow characteristics is far to be assured, aerodynamic admittance functions cannot be considered as independent on the incoming flow and the aerodynamic operator is not linear.
Since the thin airfoil theory does not apply to bluff bodies, aerodynamic admittance functions of bridge deck sections cannot be defined analytically and they are determined experimentally by wind tunnel tests (Kawatani and Kim 1992, Larose 1999, Cigada *et al* 2002). Alternatively, recent studies have introduced relationships among the aerodynamic admittance functions and the flutter derivatives (Scanlan and Jones 1999, Tubino 2004).
However, wind tunnel tests are time consuming, they do not allow to determine the complete set of aerodynamic admittance functions and experimental methods to be adopted are still under discussion. Moreover, since integral quantities such as resultant forces are commonly measured in wind tunnel, an interpretation of the results is hard to be carried out.
According to the authors of the present paper, the computational approach can contribute to shed some light on the complex problems involved in extending the aerodynamic admittance concept to bluff bodies and it could represent an efficient method to extract the complete set of aerodynamic admittance functions. In fact, on one hand, the post-processing facilities enable a deeper insight of the fluid flow phenomena occurring between the gust and the separated flow field surrounding the body. Hence, a more clear portrait of the roles played by buffeting and self-buffeting phenomena and their effects on aerodynamic admittance functions trend can be provided. On the other hand, the computational approach allows to simulate flow conditions that are hard to generate in experimental set-up. For instance, initial and boundary conditions can be imposed in order to generate incoming gust characterized by only one velocity component at a time. Hence, the complete set of the aerodynamic admittance functions can be determined. Moreover, the intensity of the incoming velocity fluctuation can be easily controlled in order to check the linear dependence of buffeting forces on the incoming flow. A first tentative to evaluate the aerodynamic admittance functions through the Computational Fluid Dynamics has been made by Turbelin (2000) by directly applying the indicial approach. The same approach has been modified by the authors of the present paper (Bruno *et al*, 2004) in order to make the method consistent with computational simulation procedures. The proposed method has been applied in conditions as close as possible to the assumptions of the thin airfoil theory and the obtained results are in good agreement with the Sears function.
In this paper the procedure is adopted for evaluating aerodynamic admittance functions relating the three generalised force components to the vertical turbulence for an aerodynamic profile with finite depth/width ratio (Naca 0012) and for the bluff section of a bridge deck (Great Belt East Bridge). A critical discussion of the obtained results is proposed in order to exploit and verify the above mentioned potentialities of the computational approach. Finally, the computed aerodynamic

admittance functions are compared with the Sears function and with wind tunnel tests results, respectively.

2. BUFFETING FORCES: AERODYNAMIC ADMITTANCE FUNCTIONS AND OVERVIEW OF THE METHODS OF EXTRACTION

Let us consider a fixed bridge deck section immersed in a 2-dimensional wind field. The field is characterised by the mean wind velocity U and the turbulence vector $\boldsymbol{V}(t)=\{u(t)\ w(t)\}^{\mathrm{T}}$, u and w being the longitudinal and the vertical turbulence components, respectively. Due to the wind action, the section is subjected to a set of generalized buffeting forces in the alongwind direction $F_x(t)$ (drag force), in the crosswind direction $F_z(t)$ (lift force) and a torsional moment $M_\theta(t)$. The vector $\boldsymbol{F}_b(t)$ of the buffeting forces per unit length acting on the segment is commonly expressed in the frequency domain as follows:

$$\boldsymbol{F}_b(\omega)=\frac{1}{2}\rho UB\boldsymbol{A}(\omega)\boldsymbol{V}(\omega)$$

$$\boldsymbol{F}_b(\omega)=\begin{Bmatrix} F_x(\omega) \\ F_z(\omega) \\ M_\theta(\omega) \end{Bmatrix} \quad ; \quad \boldsymbol{A}(\omega)=\begin{bmatrix} 2c_D\chi_{xu}(\omega) & (c'_D-c_L)\chi_{xw}(\omega) \\ 2c_L\chi_{zu}(\omega) & (c_D+c'_L)\chi_{zw}(\omega) \\ 2Bc_M\chi_{\theta u}(\omega) & Bc'_M\chi_{\theta w}(\omega) \end{bmatrix} \quad ; \quad \boldsymbol{V}(\omega)=\begin{Bmatrix} u(\omega) \\ w(\omega) \end{Bmatrix} \tag{1}$$

where ρ is the air density, B is a representative size of the deck section, c_D, c_L and c_M are the drag, lift and torsional moment static coefficients, respectively; the prime indicates a derivative with respect to the mean wind angle of attack α; $\boldsymbol{V}(\omega)$ and $\boldsymbol{F}_b(\omega)$are the vectors of the generalised Fourier transforms of $\boldsymbol{V}(t)$ and $\boldsymbol{F}_b(t)$, respectively and the functions $\chi_{\varepsilon\eta}(\omega)$ ($\varepsilon=x,\ z,\ \theta$; $\eta=u,\ w$) represent frequency-filters that transform the turbulence components into buffeting forces; their square moduli are known as aerodynamic admittance functions. The expressions for the forces in the quasi-steady theory can be obtained from Eq. (1) imposing all the aerodynamic admittance functions equal to 1.

Because of the limited experimental facilities at the beginning of sixties, Davenport (1962) evaluated the aerodynamic admittance for the drag, called velocity correlation, through an operation of average of the cross correlation of turbulence over the cross-sectional area of the section, postulated to be the region of the flow affecting the resistance of the structure. Such aerodynamic admittance function considers the lack of correlation of pressures in the region surrounding the body, but does not depend on the signature turbulence characteristics. Since the Sears function is similar to the velocity correlation, he assumed that also the aerodynamic admittance functions for lift and moment are equal to the introduced velocity correlation.

Several proposals have been made to obtain experimentally the aerodynamic admittance functions. They are commonly evaluated by wind tunnel tests on section models in turbulent flow (Larose 1999). During these tests, the power spectral density functions of the lift and of the moment are generally obtained from a direct measurement of the resultant forces. Moreover, anemometers are used to estimate the power spectral density function of the vertical turbulence component. The aerodynamic admittance functions χ_{zw} and $\chi_{\theta w}$ are then evaluated as functions of the ratio between the power spectral density function of the lift/moment and the power spectral density function of the vertical turbulence. This method can be considered as approximately valid if the contribution of the longitudinal turbulence component to the lift force and to the torsional moment can be neglected.

A different experimental approach has been proposed by different authors in order to identify separately the aerodynamic admittance functions. They are based on the active generation of one turbulent component at a time. Kawatani and Kim (1992) measured the aerodynamic admittance functions $\chi_{zu}(\omega)$ and $\chi_{zw}(\omega)$ for the lift force acting on rectangular cylinders by generating a flow characterized by only one turbulent component. Cigada *et al* (2002) evaluated the aerodynamic admittance functions $\chi_{zw}(\omega)$ and $\chi_{\theta w}(\omega)$ by means of the active generation of two harmonically

varying velocity components; analyses are carried out under the hypothesis that the generated longitudinal harmonic component is negligible with respect to the vertical one. These tests allow to evaluate the complex transfer function between the vertical turbulence component and the buffeting forces. Differently from all the other wind tunnel experiments which are carried out in turbulent flow, during these tests the incident flow is laminar and the aerodynamic behaviour observed can differ from the one detected with the other methods.
Generally speaking, such kind of experimental approaches are complex and time consuming. For this reason, the Sears function is still widely adopted in the study of the wind excited response of long span bridges (Katsuchi *et al* 1999).
A further possibility, recently proposed in literature, consists in obtaining the aerodynamic admittance functions from the flutter derivatives (Tubino 2004). However, the lack of methods for the experimental determination of the complete set of aerodynamic admittance functions does not allow the experimental validation of the proposed relationships. Moreover, the aerodynamic admittance functions so evaluated as functions of the flutter derivatives do not take into account the lack of correlation of the turbulence components in the region surrounding the body.

3. AERODYNAMIC ADMITTANCE FUNCTIONS BY CWE

In this paper, aerodynamic admittance functions relating the generalized forces to the vertical turbulence are determined in the frame of the Computational Wind Engineering through a modified indicial approach (Bruno *et al* 2004) which allows a reduction of the time extension of the numerical simulation. The method, already described and validated with reference to the thin airfoil theory, is based on the following steps:

1. computational simulation of the aerodynamic behaviour of the obstacle with steady homogeneous incoming flow at null incidence : U=1, W=0 (Figure 1a);
   i. selection of a point (x_W; z_W) in the upwind domain where the velocity field is not influenced by the presence of the body itself;
   ii. selection of the abscissa $x_0 < x_W$ in the upwind domain, which is the boundary of the sub-domain where the discontinuity $W = \overline{W}$ is imposed (Figure 1b).
2. Computational simulation of the gust propagation and of the gust-obstacle interaction (see domain and boundary/initial conditions in Figure 1b)
   i. extraction of the time history of the vertical velocity $W(t)$ in point (x_w; z_w);
   ii. integration of the surface stresses to obtain the resultant forces on the body $F_x(t)$, $F_z(t)$, $M(t)$;
3. Post processing in order to extract aerodynamic admittance function:
   i. computation of the time derivatives of the vertical velocity $\dot{W}(t)$ and of the three force components $\dot{F}_x(t)$, $\dot{F}_z(t)$ and $\dot{M}(t)$;
   ii. computation of the Fourier transforms $\dot{W}(\omega)$, $\dot{F}_x(\omega)$, $\dot{F}_z(\omega)$, $\dot{M}(\omega)$;
   iii. evaluation of the aerodynamic admittance functions $\chi_{\varepsilon w}(\omega)$ ($\varepsilon = x, z, \theta$).

The described method works for any adopted numerical approach and physical model.

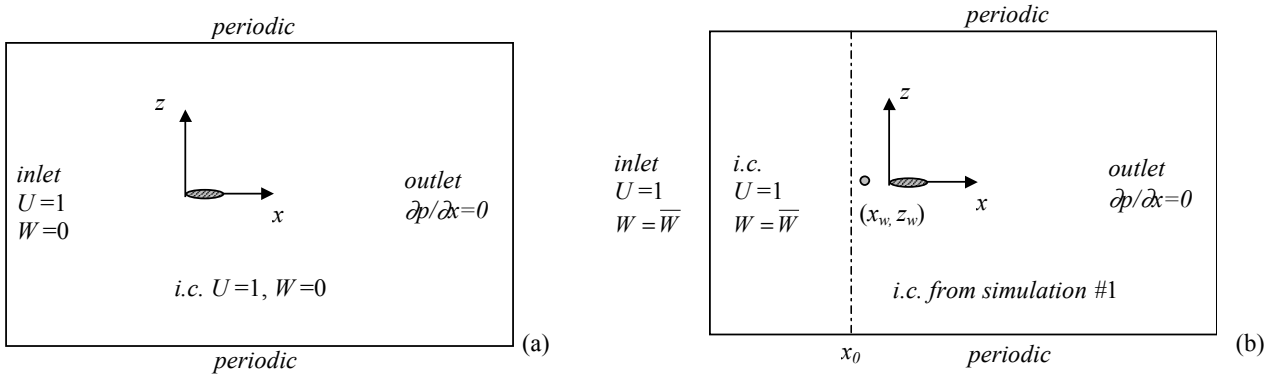

Figure 1: Set-up simulation: (a) simulation # 1, (b) simulation # 2.

4. APPLICATIONS AND RESULTS

One of the objective of this study is the evaluation of the aerodynamic admittance function in actual flows of interest for the Wind Engineering around real sections.
In order to follow a step by step approach starting from the thin plate application discussed in Bruno *et al* (2004), two sections are investigated in this paper: a streamlined body with finite depth/width ratio (Naca 0012 symmetrical wing section, B/D = 8.3) and a bluff body (the Great Belt East Bridge (GBEB) deck section, B/D = 7.2).
The former is adopted in order to discuss the effects of thickness and wall curvature on aerodynamic admittance functions with respect to the thin plate. Traditionally, such effects are disregarded and the aerodynamic admittance functions are modelled by the Sears function.The GBEB section lies in the same range of B/D ratio but its sharp edges can involve the separation of the boundary layer under certain flow conditions (quasi-streamlined or low degree-of-bluffness body). Secondly, the effects of unsymmetrical section on the gust propagation can be evaluated.
The geometry of the sections are shown in Figure 2 together with the computational grid adopted in their neighbourhood. In both computational models particular attention has been paid in order to assure suitable grid density and grid quality in the regions of interest of the computational domain. In order to manage the interface between the coarse grid for $x<x_0$ and the very fine grid for $x>x_0$, non conformal mesh has been adopted. Finally, the wall turbulent boundary layer is fully resolved by means of about 20 control volumes in the viscous sub-layer. For each section, the approach described in the previous paragraph is followed. The simulated flow fields are discussed from a physical point of view and the obtained results are compared with experimental measurements if available.

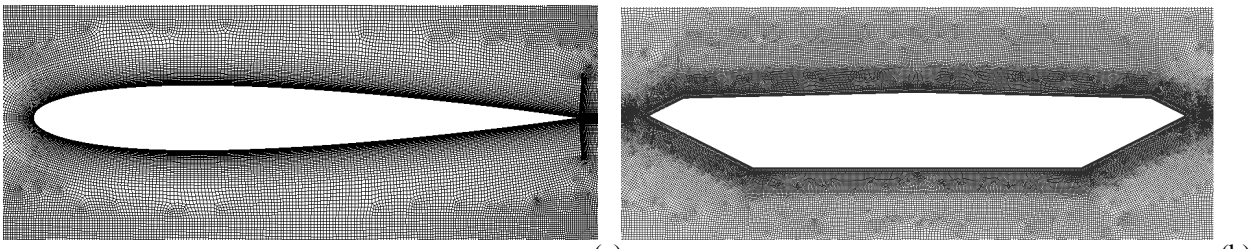

(a) (b)

Figure 2: Computational grid close to the sections: Naca0012 (a), Great Belt East Bridge deck (b).

4.1.Naca 0012

The steady state flow past the Naca 0012 profile has been simulated at angles of attack α equal to 0°, 4°, 8°, 12° in order to validate the computational results and to discuss the behaviour of the aerodynamic operator. Bearing in mind the characteristics of the flow, turbulence modelling is accomplished by means of the statistical approach (RANS equations) using the k-ε model in its RNG formulation (e.g. in Bruno and Khris 2003). The discretization procedures are the same as the ones selected in Bruno *et al* (2004).
Figure 3 compares the results of the steady computational simulation with the experimental results obtained in wind tunnel at Re = 7.6 10^5 in smooth incoming flow. Figure 3a depicts the distributions of the mean pressure coefficient C_p on the upper and lower surfaces of the profile at 0° and 4° angle of attack. The pressure distributions obtained from the numerical simulations are in good agreement with the experimental tests. Figure 3b shows the static coefficients c_D , c_L , c_M as functions of the angle of attack. A good agreement between experimental and computational results can be found for incidences $\alpha \leq 10°$, i.e. far enough from the stall condition ($\alpha \approx 13°$). In this range no fluctuations of the relevant quantities of the flow arise and the static coefficients linearly depend on the angle of attack (Figure 3b) for $0° \leq \alpha \leq 10°$. Thus, aerodynamic admittance functions are expected to be independent on the inlet flow conditions.

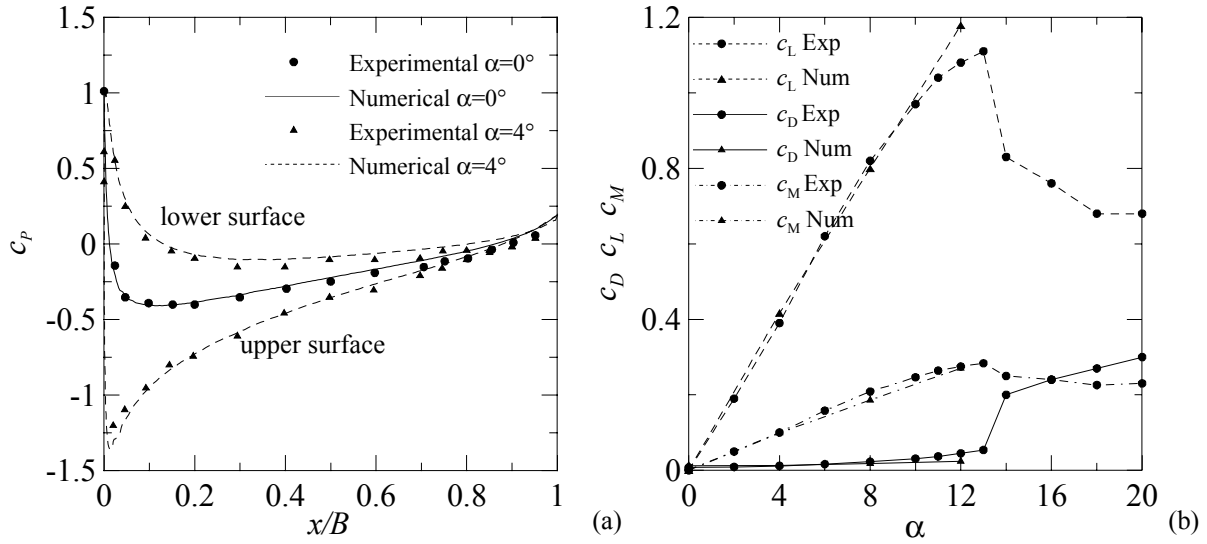

Figure 3: Steady-state flow past Naca 0012: pressure distributions and static coefficients.

The simulation of the gust propagation past the obstacle is accomplished in the same conditions employed for the thin plate in Bruno *et al* 2004 (Re=10^4). Figure 4 compares the computational results obtained for both streamlined bodies with the closed form solution given in the frame of the thin airfoil theory. In particular, Figure 4a shows the time history of the vertical component of the velocity W and the smoothed step response function $C_L/C_{L\infty}$. The diagrams refer to a short extent of the reduced time around $\tau = t\text{-}t_L = 0$, t_L being the time when the gust boundary reaches the leading edge. In Figure 4b the aerodynamic admittance function for the lift χ_L is plotted versus the reduced frequency $f_r = nB/U$. Differences between the thin airfoil case and the thick one (Naca0012) can be observed for $f_r > 1$, i.e. for $n > 1/B$ or $\lambda < B$, being $\lambda \propto U/B$ the wavelength of the incoming eddies. It can be deduced that the lift force acting on the Naca profile is less sensitive than thin plate to effects of cross correlation of velocity fluctuation over the cross-sectional area of the section. Looking at the flow field close to the wing, it can be observed that the velocity gradients due to the wall curvature are higher that those involved by the gust; thus, the wall boundary layer is stably driven by the curvature effects. On the contrary, the effect of the gust remains relevant in the wake, that is for eddies with a wave length larger than the chord of the wing ($\lambda < B$, i.e. $f_r > 1$).

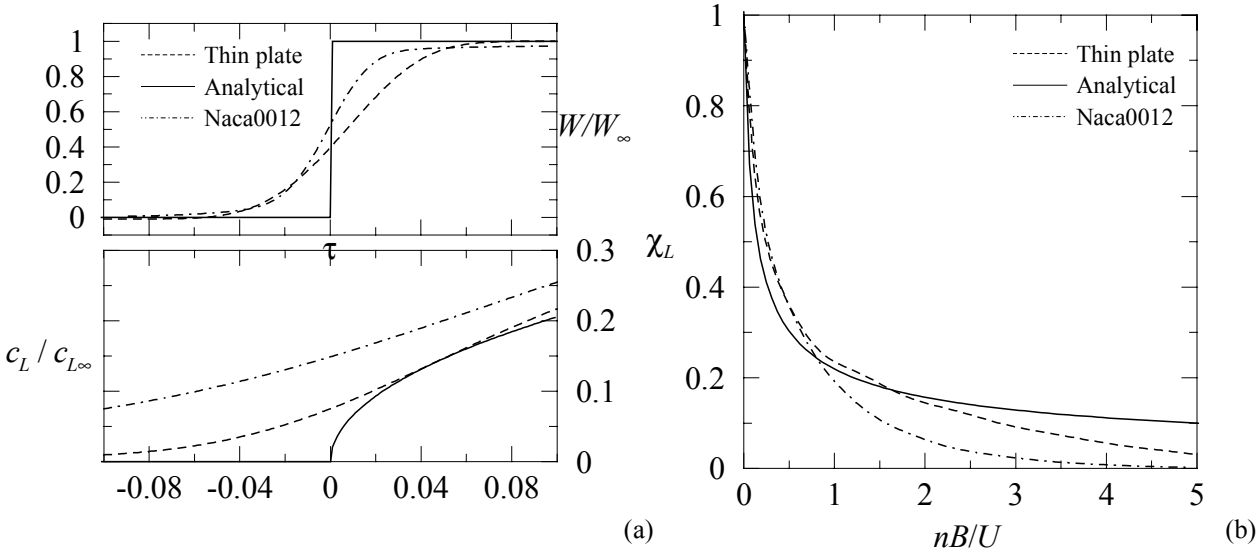

Figure 4: Naca 0012: Time histories and aerodynamic admittance function for the lift.

Figure 5 shows the time histories of drag, lift and moment (Figure 5a) and the corresponding aerodynamic admittance functions (Figure 5b). Aerodynamic admittance functions for lift and moment are coincident. The difference observed for drag can be easily explained according to the physical interpretation given above. In fact, the drag acting on streamlined bodies is mainly due to

the friction component, which is strongly influenced by the boundary layer characteristics, i.e. by the curvature of the profile. It follows that the drag sensitivity to gust effects is weaker than the one shown by the other force components. Thus, the unit value of its aerodynamic admittance function at $f_r = 0$ quickly decreases as reduced frequency increases.

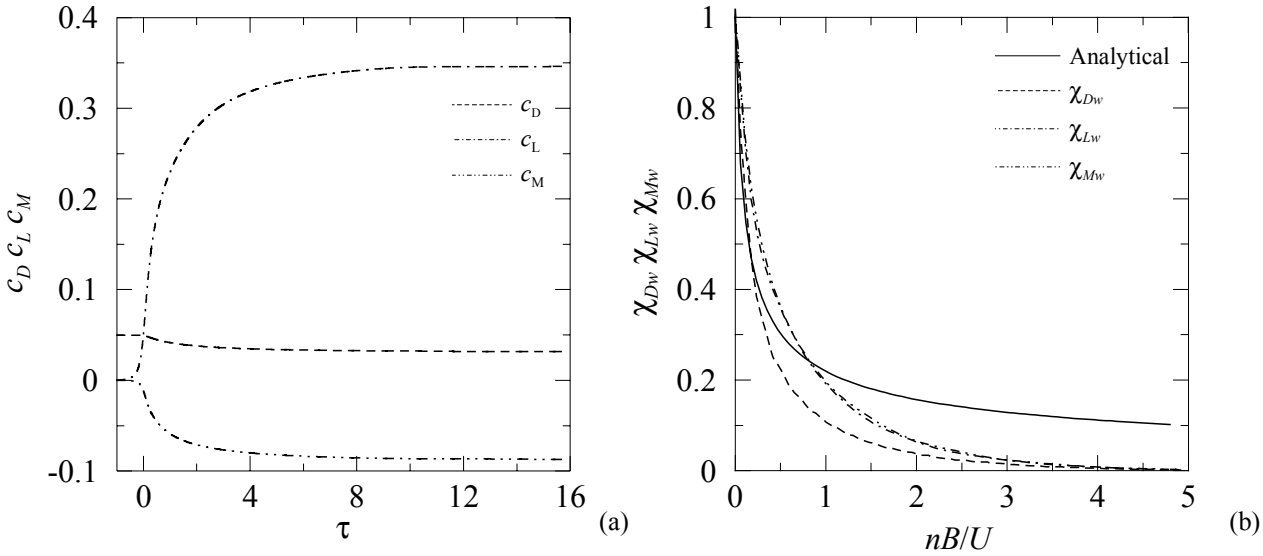

Figure 5: Naca 0012: Time histories and aerodynamic admittance function for drag, lift and moment.

4.2.Great Belt East Bridge

The simulation of the complex unsteady flow past the Great Belt East Bridge deck is accomplished by means of Large Eddy Simulation approach to turbulence and requires particular care in the choice of the discretization procedures. Being the description of the optimisation of the computational model out of the scope of this paper, the reader can refer to Bruno and Khris (2003). Just a few number of results are reported here to state the level of accuracy of the simulation. Bearing in mind that the flow around bluff bodies is mainly characterised by boundary layer separation, the key point of its prediction lies in the simulation of the structures of the flow responsible of boundary layer detachment and reattachment. Figure 6 compares the flow structures experimentally observed by Pullin and Perry (Buresti 1998) with the instantaneous topology of the flow simulated by CWE. Both visualizations highlight the same structures, while discrepancies in their shape are clearly due to the differences in edge geometries and flow conditions.

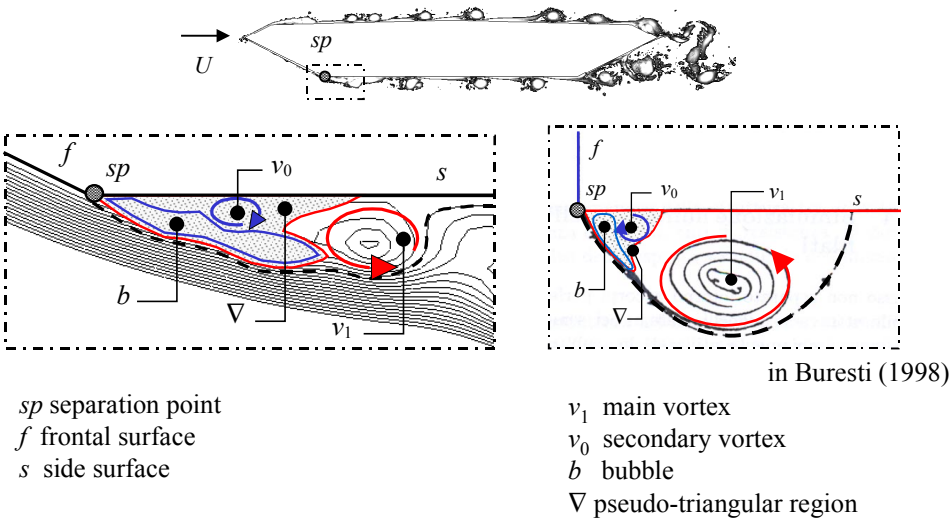

in Buresti (1998)

sp separation point
f frontal surface
s side surface

v_1 main vortex
v_0 secondary vortex
b bubble
∇ pseudo-triangular region

Figure 6: Great Belt East Bridge: flow structures past separation point superimposed to instantaneous streamlines

Because of the strong unsteadiness of the flow, accuracy of the computational prediction is required with respect to both mean quantities and instantaneous ones. Figure 7a compares the mean pressure distributions at α=0° obtained by computational simulations (Bruno and Khris 2003, Re=10^5) with the data measured on taut strip model in turbulent flow (Larose 1992, Re = 7 10^4, turbulence intensity Iu = 7.5%) and on a section model in smooth flow (Reinhold *et al* 1992, Re= 10^5). The computational results show an overall good agreement with the experimental measurements. Figure 7b shows the power spectral density function of the lift force obtained by CWE and compares it with the Strouhal numbers evaluated in wind tunnel tests. Coherently with flow visualizations, various spikes can be observed in power spectral density function, which are related to different vortex shedding mechanisms. Hence, the corresponding signature turbulence induced by the body cannot be modelled as a classical Von Karman vortex shedding characterised by only one harmonic component.

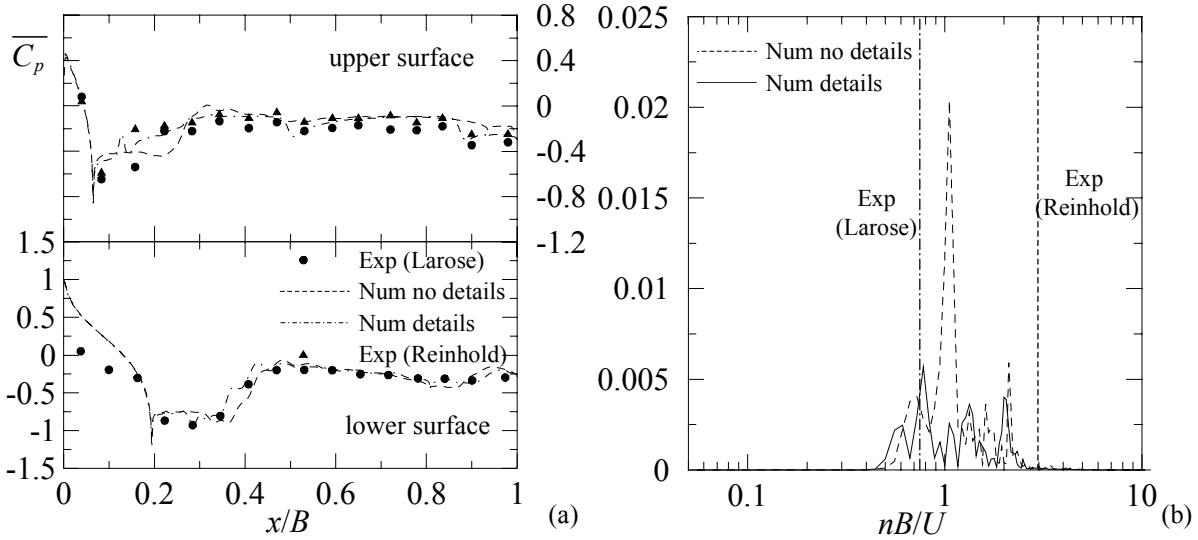

Figure 7: Great Belt East Bridge: mean pressure distribution (a) and power spectral density function of the lift (b) at α=0°

Two numerical simulations of the propagation of a gust of amplitude $\overline{W} = 3.5\%U$ and $\overline{W} = 7\%U$ across the bare section have been carried out in order to discuss the linearity of the aerodynamic operator. Figure 8 shows the results obtained from both simulations. Figures 8a and 8b depict, respectively, the time histories of drag, lift and moment with the two gust amplitudes and the corresponding aerodynamic admittance functions. From Figure 8a, it can be observed that the time variations of the forces due to the self buffeting are of the same order of magnitude as the variation due to the smoothed gust. The great influence of the signature turbulence on the aerodynamic forces arising on the section can be recognized also in Figure 8b, where significant spikes much greater than unit can be seen in the aerodynamic admittance functions. From Figure 8b, it can be observed that the aerodynamic admittance functions obtained from the two simulations with different gust amplitudes do not coincide. Hence, the linearity of the aerodynamic operator mapping the incident turbulence component into the force components does not hold and the representation of the buffeting forces through aerodynamic admittance functions could not be suitable for bluff bodies.

A simulation of the propagation of a gust with amplitude $\overline{W} = 7\%U$ past the bridge deck section with barriers has been performed in order to allow a comparison with available experimental data. Figure 9 compares the numerical results with the experimental ones. In Figure 9a, the aerodynamic admittance functions for lift and moment obtained numerically are compared with the ones evaluated experimentally by Larose (1999). The numerically evaluated aerodynamic admittance functions are much greater than the experimental ones. These discrepancies are probably due to the differences in the incoming flow conditions: the experimental tests are performed in incoming turbulent flow, while the modified indicial approach proposed here allows numerical simulations of

a deterministic smoothed gust in incoming smooth flow. For this kind of low degree-of-bluffness section, the turbulent nature of the wall boundary layer induced by inlet flow turbulence can avoid separation and deeply reduce or inhibit vortex shedding. Hence, the effect of signature turbulence on the experimentally evaluated aerodynamic admittance function is much less evident. The above mentioned effect generally does not take place for high degree-of-bluffness section: an example is given in Figure 9b, comparing the lift aerodynamic admittance function numerically evaluated for the GBEB with the one estimated from wind tunnel tests in turbulent flow for a rectangular cylinder with *B/D*=5 (Kawatani and Kim 1992). In both cases, the aerodynamic admittance functions show spikes. The spikes corresponding to *B/D*=5 section are at frequencies lower than the ones corresponding to the GBEB (*B/D*=7.2) in accordance with the general trend of the Strouhal number versus *B/D* ratio for rectangular sections.

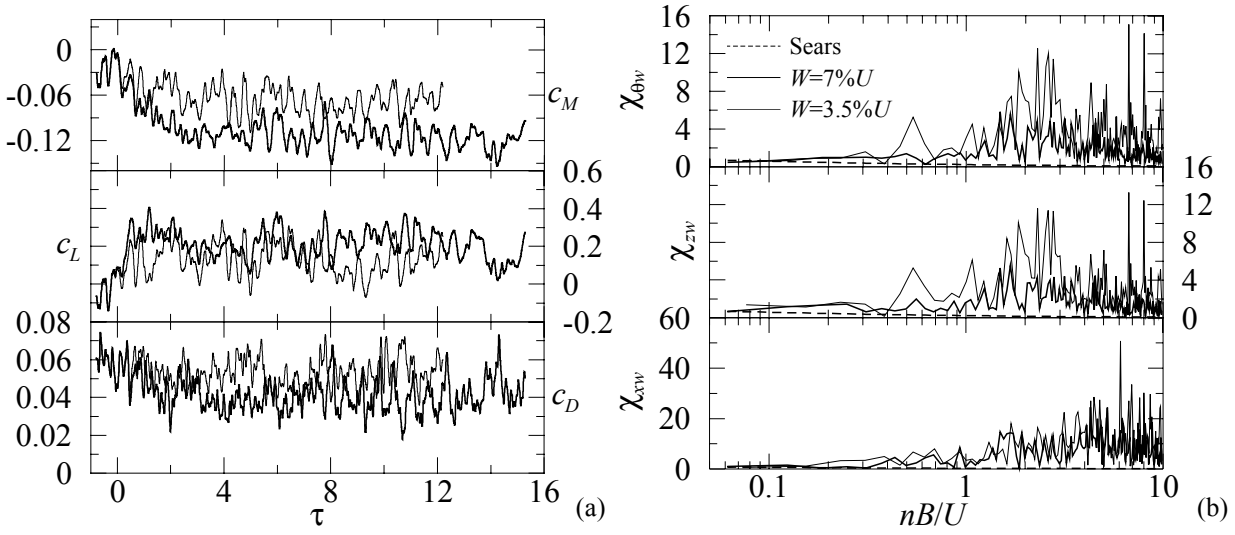

Figure 8: Time histories of the forces (a) and aerodynamic admittance functions (b).

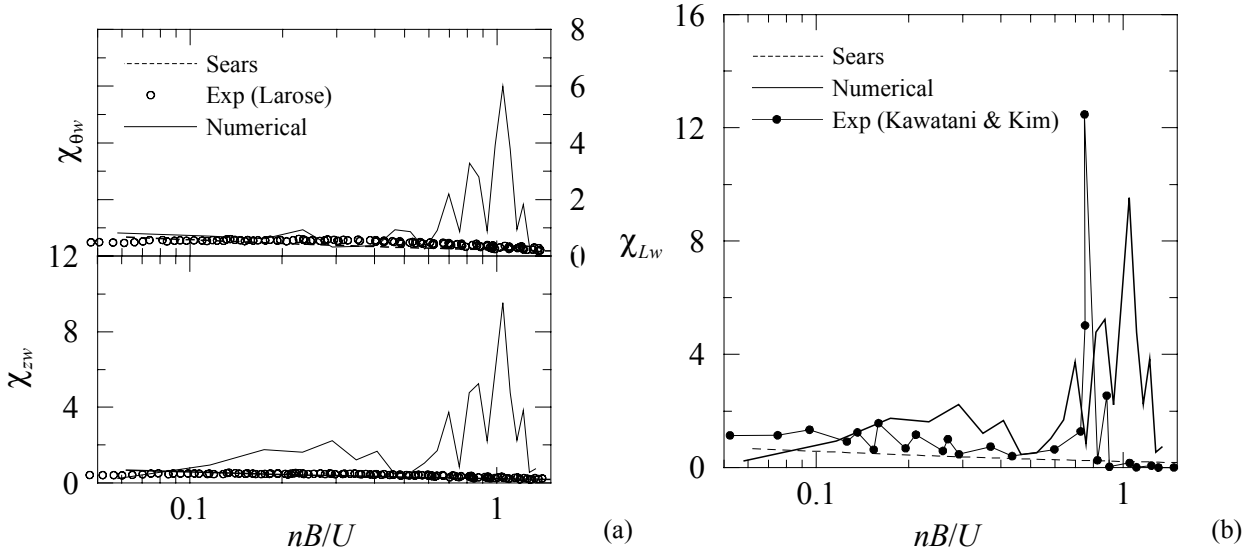

Figure 9: Comparison among numerically and experimentally evaluated aerodynamic admittance functions.

5. CONCLUSIONS AND PROSPECTS

In this paper, the aerodynamic admittance functions for a streamlined and a bluff body have been evaluated by CWE.

The numerically estimated aerodynamic admittance functions of thick streamlined bodies are different from the Sears function: the aerodynamic admittance functions for lift and moment are

lower than the Sears function in the high frequency range, while the aerodynamic admittance function for the drag is lower than the Sears function at every frequency. From a design point of view using the Sears function leads to a conservative design of structures.
More relevant differences are observed concerning the aerodynamic admittance functions of the Great Belt East Bridge deck section. On the one hand, the obtained results show a dominant contribution of the signature turbulence. On the other hand, the comparison between the numerical results and the aerodynamic admittance functions experimentally evaluated in turbulent flow conditions highlights the strong sensitivity of buffeting forces to the inlet flow conditions. That is probably due to the relevant dependence of vortex shedding mechanism around low degree-of-bluffness bodies from Reynolds number and incoming turbulence intensity. Moreover, the dependence of the aerodynamic admittance function on the gust amplitude emphasises the non-linearity of the aerodynamic operator mapping the vertical turbulence into the aerodynamic forces. From a design point of view using the Sears function for more or less bluff bodies can lead to unsafe design conditions.
As a prospect of this work, the comparison of the numerical results with experimental data obtained in the same flow conditions seems necessary in order to fully evaluate the accuracy of the proposed approach in bluff body aerodynamics. Further efforts in research seem to be required in order to formulate an aerodynamic operator more suitable for bluff body aerodynamics.

ACKNOWLEDGMENTS

The authors wish to express their grateful acknowledgment to the L3M - Laboratoire de Modélisation et Simulation Numérique en Mécanique – Marseille - France for the kind availability of the computing facilities.

6. REFERENCES

Bruno L., Khris S. (2003), On the validity of 2D numerical simulations of vortical structures around a bridge deck, *Mathematical and Computer Modelling*, vol. 37, 7/8, pp. 795-828.

Bruno L., Tubino F., Solari G. (2004), Aerodynamic admittance functions of streamlined bodies: the indicial approach by CWE, IN-VENTO 2004, Reggio Calabria.

Buresti G. (1998), Vortex-shedding from bluff bodies. *Wind effects on buildings and structures*, Balkema, Rotterdam.

Cigada A., Diana G., Zappa E. (2002), On the response of a bridge deck to turbulent wind: a new approach, *J. Wind Engng and Ind. Aerodynamics*, Vol. 90, pp. 1173-1182.

Davenport A.G. (1962), Buffeting of a suspension bridge by storm winds, *J. Struct. Division ASCE*, Vol. 88-3, pp. 233-268.

Fung Y.C. (1993), *An introduction to the theory of aeroelasticity*, Dover Publications, New York, U.S.A.

Katsuchi H., Jones N.P. and Scanlan R.H. (1999), Multimode coupled flutter and buffeting analysis of the Akashi-Kaikyo bridge, *J. Struct. Engng ASCE*, Vol. 125(1), pp. 60-70.

Kawatani M., Kim H. (1992), Evaluation of aerodynamic admittance for buffeting analysis, *J. Wind Engng and Ind. Aerodynamics*, Vol. 41-44, pp. 613-624.

Larose G.L. (1999), Experimental determination of the aerodynamic admittance of a bridge deck section, *J. Fluids and Structures*, Vol. 13, pp. 1029-1040.

Larose G.L. (1992), The response of a suspension bridge deck to the turbulent wind: the taut-strip model approach, M. Eng. Sc. The University of Western Ontario. Ontario.

Reinhold T.A., Brinch M. and Damsgaard A. (1992), Wind tunnel tests for the Great Belt Link, *Proc. Int. Symp. on Aerodynamics of Larges Bridges*, Larsen (Ed.), Balkema, Rotterdam, pp. 255-268.

Sears W.R. (1941), Some aspects of non-stationary airfoil theory and its practical application, *J. Aero. Sci.*, Vol. 8(3), pp. 104-108.

Tubino F. (2004), Aerodynamic and aeroelastic actions on long-span bridges, *J. Wind Engng and Ind. Aerodynamics*, submitted.

Turbelin G. (2000), Modélisation de la turbulence atmosphérique en vue de l'étude du chargement aérodynamique des structures soumises aux effets du vent, PhD Thesis, Université d'Evry Val d'Essonne, France.